Atmospheric Chemistry of $CF_3CH_2CH_2OH$: Kinetics, Mechanisms and Products of Cl Atom and OH Radical Initiated Oxidation in the Presence and Absence of NO_X

Michael D. Hurley,* Jessica A. Misner, James C. Ball, and Timothy J. Wallington
Ford Motor Company, Mail Drop SRL-3083, Dearborn, Michigan 48121

D. A. Ellis, J. W. Martin, and S. A. Mabury
Department of Chemistry, 80 St. George Street, University of Toronto, Toronto, Ontario, Canada M5S 3H6

M. P. Sulbaek Andersen
Department of Chemistry, University of Copenhagen, Universitetsparken 5, DK 2100 Copenhagen, Denmark

Received: June 30, 2005; In Final Form: September 1, 2005

Relative rate techniques were used to study the kinetics of the reactions of Cl atoms and OH radicals with $CF_3CH_2C(O)H$ and $CF_3CH_2CH_2OH$ in 700 Torr of N_2 or air diluent at 296 ± 2 K. The rate constants determined were $k(Cl+CF_3CH_2C(O)H) = (1.81 \pm 0.27)$ x 10^{-11}, $k(OH+CF_3CH_2C(O)H) = (2.57 \pm 0.44)$ x 10^{-12}, $k(Cl+CF_3CH_2CH_2OH) = (1.59 \pm 0.20)$ x 10^{-11}, and $k(OH+CF_3CH_2CH_2OH) = (6.91 \pm 0.91)$ x 10^{-13} cm^3 $molecule^{-1}$ s^{-1}. Product studies of the chlorine initiated oxidation of $CF_3CH_2CH_2OH$ in the absence of NO show the sole primary product to be $CF_3CH_2C(O)H$. Product studies of the chlorine initiated oxidation of $CF_3CH_2CH_2OH$ in the presence of NO show the primary products to be $CF_3CH_2C(O)H$ (81%), HC(O)OH (10%), and $CF_3C(O)H$. Product studies of the chlorine initiated oxidation of $CF_3CH_2C(O)H$ in the absence of NO show the primary products to be $CF_3C(O)H$ (76%), $CF_3CH_2C(O)OH$ (14%), and $CF_3CH_2C(O)OOH$ (≤10%). As part of this work, an upper limit of $k(O_3+CF_3CH_2CH_2OH) < 2 \times 10^{-21}$ cm^3 $molecule^{-1}$ s^{-1} was established. Results are discussed with respect to the atmospheric chemistry of fluorinated alcohols.

1. Introduction

Fluorinated alcohols are used in a variety of industrial applications (e.g., paints, coatings, polymers, adhesives, waxes, polishes, electronic materials, caulks). In light of the widespread use of fluorinated alcohols, detailed information on their environmental impact is needed. There is a concern, for example, that atmospheric oxidation processes convert fluorinated alcohols to perfluorinated carboxylic acids (PFCAs) of the form $C_nF_{2n+1}C(O)OH$. PFCAs are persistent in the environment, resisting degradation via oxidation, hydrolysis, or reduction under biotic and abiotic conditions.[1] Analysis of rainwater indicates the widespread distribution of short-chain PFCAs ($n = 2-7$) at low levels (~1−100 ng/L).[2] PFCAs are bioaccumulative in fish when the perfluorinated chain is more than seven carbons in length.[3] Long-chain PFCAs ($n = 7-14$) have been observed in fish from the Great Lakes[4] and in Arctic fish and mammals.[5] Perfluorooctanoic acid (PFOA), is potentially toxic,[6−8] and the health effects associated with long-term exposure to PFOA are the subject of a current risk assessment.[9]

Fluorotelomer alcohols (FTOHs) are a class of fluorinated alcohols that have been suggested as plausible sources of PFCAs in remote locations.[10,11] FTOHs are linear fluorinated alcohols with the formula $F(CF_2)_nCH_2CH_2OH$ (n = 2, 4, 6, ...). Fluorotelomer alcohols are volatile, appear to be ubiquitous in the North American atmosphere (17−135 pg m^{-3}),[12,13] have an atmospheric lifetime (approximately 10−20 days) sufficient for widespread hemispheric distribution,[10,14] and undergo atmospheric oxidation in the absence of NO_X to give perfluorocarboxylic acids.[11,15] To improve our understanding of the atmospheric chemistry of fluorinated alcohols in general and fluorotelomer alcohols in particular, $CF_3CH_2CH_2OH$ and the expected oxidation product, $CF_3CH_2C(O)H$, were studied using the smog chamber at the Ford Motor Co. The kinetics and mechanism of their simulated atmospheric oxidation was monitored using Fourier transform infrared spectroscopy (FTIR) and the results are reported here.

2. Experimental Section

Experiments were performed in a 140 L Pyrex reactor interfaced to a Mattson Sirius 100 FTIR spectrometer.[16] The reactor was surrounded by 22 fluorescent blacklamps (GE F15T8-BL), which were used to photochemically initiate the experiments. Chlorine atoms were produced by photolysis of molecular chlorine.

$$Cl_2 + h\nu \rightarrow Cl + Cl \qquad (1)$$

OH radicals were produced by the photolysis of CH_3ONO in air:

$$CH_3ONO + h\nu \rightarrow CH_3O + NO \qquad (2)$$

$$CH_3O + O_2 \rightarrow HO_2 + HCHO \qquad (3)$$

$$HO_2 + NO \rightarrow OH + NO_2 \qquad (4)$$

Relative rate techniques were used to measure the rate constant of interest relative to a reference reaction whose rate constant

---

* Corresponding author. E-mail: mhurley3@ford.com.

10.1021/jp0535902 CCC: $30.25

has been established previously. The relative rate method is a well-established technique for measuring the reactivity of Cl atoms and OH radicals with organic compounds.[17] Kinetic data are derived by monitoring the loss of a reactant compound relative to one or more reference compounds. The decays of the reactant and reference are then plotted using the expression

$$\ln\left(\frac{[\text{reactant}]_{t_0}}{[\text{reactant}]_t}\right) = \frac{k_{\text{reactant}}}{k_{\text{reference}}}\ln\left(\frac{[\text{reference}]_{t_0}}{[\text{reference}]_t}\right) \qquad \text{(I)}$$

where $[\text{reactant}]_{t_0}$, $[\text{reactant}]_t$, $[\text{reference}]_{t_0}$, and $[\text{reference}]_t$ are the concentrations of reactant and reference at times "t_0" and "t", k_{reactant} and $k_{\text{reference}}$ are the rate constants for reactions of Cl atoms or OH radicals with the reactant and reference. Plots of $\ln([\text{reactant}]_{t_0}/[\text{reactant}]_t)$ versus $\ln([\text{reference}]_{t_0}/[\text{reference}]_t)$ should be linear, pass through the origin, and have a slope of $k_{\text{reactant}}/k_{\text{reference}}$.

The loss of $CF_3CH_2C(O)H$ and $CF_3CH_2CH_2OH$ was monitored by FTIR spectroscopy using an infrared path length of 27 m and a resolution of 0.25 cm^{-1}. Infrared spectra were derived from 32 co-added interferograms. All experiments were performed at 700 Torr and 296 ± 2 K. Liquid reagents or reference compounds were introduced into the chamber by transferring the vapor above the liquid via a calibrated volume. Similarly, gaseous reagents were introduced into the chamber via a calibrated volume. The contents of the calibrated volume were swept into the chamber with the diluent gas (air or nitrogen). The reagents obtained from commercial sources were $CF_3CH_2C(O)H$ (SynQuest Labs, 97% min), $CF_3CH_2CH_2OH$ (SynQuest Labs, 97% min), and $CF_3CH_2C(O)OH$ (Aldrich, 98%). The peracid, $CF_3C(O)OOH$, was prepared as described previously.[18] All reagents were subjected to repeated freeze/pump/thaw cycling before use. Ultra-high-purity synthetic air and nitrogen from Michigan Airgas were used as diluent gases.

Initial reagent concentrations for Cl atom relative rate experiments were 8−10 mTorr of $CF_3CH_2C(O)H$, 15−30 mTorr of $CF_3CH_2CH_2OH$, 3−7 mTorr of the reference compound CH_3OH, 15 mTorr of the reference compound CH_3CH_2Cl, and 100−110 mTorr of Cl_2 in 700 Torr of N_2 diluent. Initial reagent concentrations for OH radical relative rate experiments were 15 mTorr of $CF_3CH_2C(O)H$, 15 mTorr of $CF_3CH_2CH_2OH$, 3−4 mTorr of the reference compound (C_2H_2 or C_2H_4), and 100 mTorr of CH_3ONO in 700 Torr of air diluent. Initial reagent concentrations for Cl atom initiated oxidation experiments were 15−22 mTorr $CF_3CH_2C(O)H$, 15−30 mTorr $CF_3CH_2CH_2OH$, and 100 mTorr Cl_2 in 700 Torr of air diluent. Reactant and reference compounds were monitored using absorption features over the following wavenumber ranges (cm^{-1}): $CF_3CH_2CH_2OH$, 3600−3700; $CF_3CH_2C(O)H$, 1700−1800; C_2H_5Cl, 600−700; CH_3OH, 1000−1100; C_2H_2, 700−800; C_2H_4, 900−1000. The time required to record a spectrum was 90 s for all experiments. The total photolysis time for the Cl relative rate experiments was 8−33 s. The total time of the Cl initiated kinetic experiments was 17−36 min. The total photolysis time for the OH relative rate experiments was 6−25 min. The total time of the OH initiated kinetic experiments was 32−53 min. In the relative rate experiments, plots of $\ln([\text{reactant}]_{t_0}/[\text{reactant}]_t)$ versus $\ln([\text{reference}]_{t_0}/[\text{reference}]_t)$ were linear and passed through the origin. Consistent kinetic data were obtained using two different reference compounds. Such behavior suggests that the present work is free of complications associated with spectral interferences or unwanted secondary reactions.

In smog chamber experiments it is important to check for unwanted loss of reactants and products via photolysis, dark chemistry, and heterogeneous reactions. Control experiments were performed in which mixtures of reactants (except Cl_2) were subjected to UV irradiation for 15−30 min, and product mixtures obtained after the UV irradiation of reactant mixtures were allowed to stand in the dark in the chamber for 15 min. There was no observable loss of reactants or products, suggesting that photolysis, dark chemistry, and heterogeneous reactions are not a significant complication in the present work. Unless stated otherwise, quoted uncertainties are two standard deviations from least squares regressions.

3. Results

The focus of this study is the atmospheric chemistry of $CF_3CH_2CH_2OH$. The atmospheric oxidation of $CF_3CH_2CH_2OH$ is expected to give the aldehyde $CF_3CH_2C(O)H$ as the primary product. As part of this work a study of the kinetics, mechanism, and products of the oxidation of the aldehyde $CF_3CH_2C(O)H$ was conducted. Results for $CF_3CH_2C(O)H$ are presented first.

3.1. Relative Rate Study of the Reaction of Cl Atoms with $CF_3CH_2C(O)H$. The kinetics of reaction 5 were measured relative to reactions 6 and 7. The top panel in Figure 1 shows

$$Cl + CF_3CH_2C(O)H \rightarrow \text{products} \qquad (5)$$

$$Cl + CH_3CH_2Cl \rightarrow \text{products} \qquad (6)$$

$$Cl + CH_3OH \rightarrow \text{products} \qquad (7)$$

the loss of $CF_3CH_2C(O)H$ versus the loss of the reference compounds following the UV irradiation of $CF_3CH_2C(O)H$/reference/Cl_2 mixtures in 700 Torr of N_2 diluent. N_2 was used as a diluent to avoid the possibility of OH generation. The lines through the data in Figure 1 are linear least-squares fits to the combined data sets that give $k_5/k_6 = 2.35 \pm 0.20$ and $k_5/k_7 = 0.32 \pm 0.04$. Using $k_6 = 7.9 \times 10^{-12}$ cm^3 $molecule^{-1}$ s^{-1} [19,20] and $k_7 = 5.5 \times 10^{-11}$ cm^3 $molecule^{-1}$ s^{-1},[21] we derive $k_5 = (1.86 \pm 0.16) \times 10^{-11}$ and $(1.76 \pm 0.22) \times 10^{-11}$ cm^3 $molecule^{-1}$ s^{-1}. Results obtained using the two different reference compounds were, within the experimental uncertainties, indistinguishable. We cite a final value for k_5 that is the average of the two determinations together with error limits that encompass the extremes of the individual determinations, $k_5 = (1.81 \pm 0.27) \times 10^{-11}$ cm^3 $molecule^{-1}$ s^{-1}. Kelly et al.[22] used the relative rate technique to measure the reactivity of Cl toward $CF_3CH_2C(O)H$ relative to $HC(O)OC_2H_5$ and report $k_5 = (2.57 \pm 0.04) \times 10^{-11}$ cm^3 $molecule^{-1}$ s^{-1}. The value of k_5 measured in the present work is 30% lower than that reported by Kelly et al.[22]

The experimental techniques used in the present work and by Kelly et al.[22] are very similar, and the 30% discrepancy between the measured values of k_5 deserves comment. In the present work the reactivity of $CF_3CH_2C(O)H$ toward Cl atoms was measured relative to the reactivity of CH_3CH_2Cl and CH_3OH. There have been numerous absolute and relative rate studies of the reactivity of CH_3CH_2Cl and CH_3OH toward Cl atoms, and k_6 and k_7 are well established. Indistinguishable values of k_5 were obtained from separate experiments employing CH_3CH_2Cl and CH_3OH references. The fact that independent experiments give consistent results provides confidence in the value of k_5 measured in the present work. In contrast, Kelly et al.[22] employed just one reference compound; $HC(O)OC_2H_5$ (ethyl formate) and the reference rate constant used by Kelly et al.[22] is based upon just one study: the work by Notario et al.,[23] which is the only study of $k(Cl+HC(O)OC_2H_5)$ reported to date.

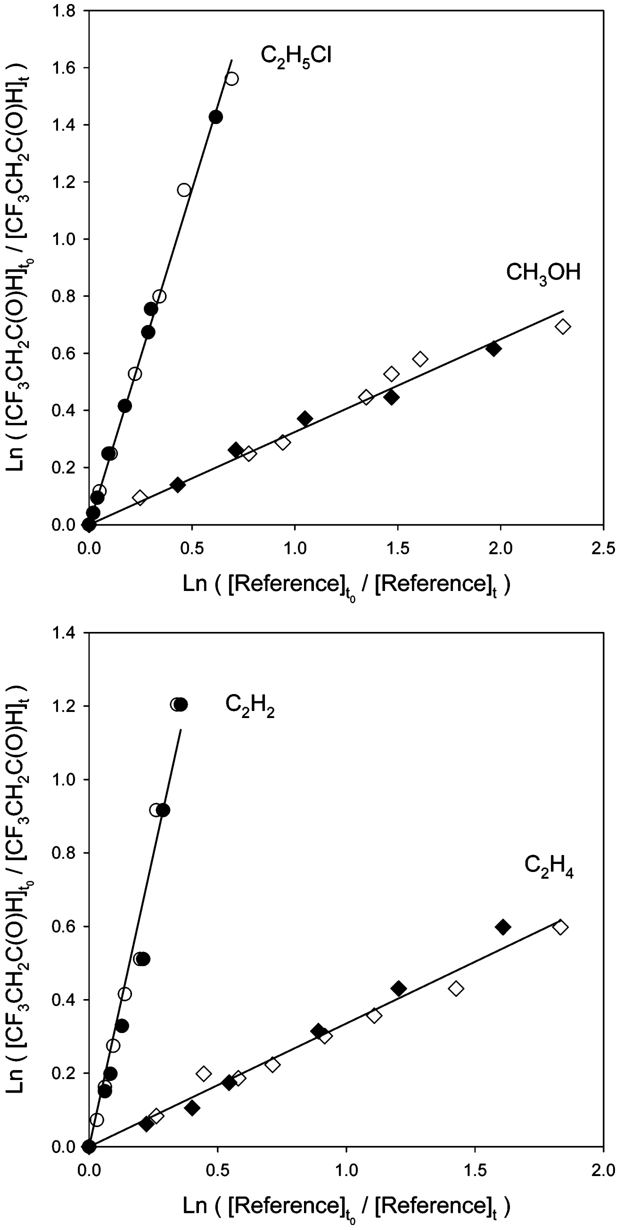

Figure 1. Top panel: loss of $CF_3CH_2C(O)H$ versus C_2H_5Cl (circles) and CH_3OH (diamonds) following UV irradiation of $CF_3CH_2C(O)H$/reference/Cl_2 mixtures in 700 Torr of N_2. Bottom panel: loss of $CF_3CH_2C(O)H$ versus C_2H_2 (circles) and C_2H_4 (diamonds) following UV irradiation of $CF_3CH_2C(O)H$/reference/CH_3ONO mixtures in 700 Torr of air.

Notario et al.[23] studied the reactivity of Cl atoms toward a series of esters. Unfortunately, recent work has cast doubt upon the results reported by Notario et al.[23]

Cavalli et al.[24] determined a value of *k*(Cl + methyl propionate) that was 24% lower than that reported in the work by Notario et al.[23] Christensen et al.[25] measured a value for *k*(Cl+methyl acetate) that was 23% lower than that reported by Notario et al.[23] Langer et al.[26] measured a value of *k*(Cl+*tert*-butyl acetate) that was 34% lower than that reported by Notario et al.[23] Finally, Wallington et al.[27] measured a value of *k*(Cl+methyl formate) that was 23% lower than that reported by Notario et al.[23] It appears that Notario et al.[23] systematically overestimated the reactivity of Cl atoms toward esters by approximately 20−30%.

We conclude that the discrepancy between values of k_5 derived in the present and previous work probably reflects errors in the reference rate constant, $k(Cl+HC(O)OC_2H_5)$, used in the previous work.[22]

3.2. Relative Rate Study of the Reaction of OH Radicals with $CF_3CH_2C(O)H$. The kinetics of reaction 8 were measured relative to reactions 9 and 10.

$$OH + CF_3CH_2C(O)H \rightarrow products \tag{8}$$

$$OH + C_2H_2 \rightarrow products \tag{9}$$

$$OH + C_2H_4 \rightarrow products \tag{10}$$

The bottom panel in Figure 1 shows loss of $CF_3CH_2C(O)H$ versus loss of the reference compounds following the UV irradiation of $CF_3CH_2C(O)H$/reference/CH_3ONO mixtures in 700 Torr air diluent. The lines through the data in Figure 1 are linear least-squares fits to the combined data sets that give $k_8/k_9 = 3.18 \pm 0.35$ and $k_8/k_{10} = 0.336 \pm 0.045$. Using $k_9 = 7.8 \times 10^{-13}$ [28] and $k_{10} = 7.9 \times 10^{-12}$,[28] we derive $k_8 = (2.48 \pm 0.27) \times 10^{-12}$ and $(2.65 \pm 0.36) \times 10^{-12}$ cm^3 $molecule^{-1}$ s^{-1}. Results obtained using the two different reference compounds were, within the experimental uncertainties, indistinguishable. We cite a final value for k_{10} that is the average of the two determinations together with error limits that encompass the extremes of the individual determinations, $k_8 = (2.57 \pm 0.44) \times 10^{-12}$ cm^3 $molecule^{-1}$ s^{-1}. Sellevåg et al.[29] used relative rate techniques to measure $k(OH+CF_3CH_2C(O)H)$ and report $k_8 = (3.6 \pm 0.3) \times 10^{-12}$ cm^3 $molecule^{-1}$ s^{-1}. Kelly et al.[22] used LP-LIF absolute rate techniques to establish $k_8 = (2.96 \pm 0.04) \times 10^{-12}$ cm^3 $molecule^{-1}$ s^{-1}. The value of $k(OH+CF_3CH_2C(O)H)$ determined in the present work is in agreement with that from Kelly et al.[22] but 30% lower than that reported by Sellevåg et al.[29] The origins of this discrepancy are unclear.

3.3. Relative Rate Study of the Reaction of Cl Atoms with $CF_3CH_2CH_2OH$. The kinetics of reaction 11 were measured relative to reactions 6 and 7.

$$Cl + CF_3CH_2CH_2OH \rightarrow products \tag{11}$$

The top panel in Figure 2 shows loss of $CF_3CH_2CH_2OH$ versus loss of the reference compounds following the UV irradiation of $CF_3CH_2CH_2OH$/reference/Cl_2 mixtures in 700 Torr of N_2 diluent. The lines through the data in Figure 2 are linear least-squares fits to the combined data sets that give $k_{11}/k_6 = 1.96 \pm 0.15$ and $k_{11}/k_7 = 0.295 \pm 0.030$. Using $k_6 = 7.9 \times 10^{-12}$ [19,20] and $k_7 = 5.5 \times 10^{-11}$,[21] we derive $k_{11} = (1.55 \pm 0.12) \times 10^{-11}$ and $(1.62 \pm 0.17) \times 10^{-11}$ cm^3 $molecule^{-1}$ s^{-1}. Results obtained using the two different reference compounds were, within the experimental uncertainties, indistinguishable. We cite a final value for k_{11} that is the average of the two determinations together with error limits that encompass the extremes of the individual determinations, $k_{11} = (1.59 \pm 0.20) \times 10^{-11}$ cm^3 $molecule^{-1}$ s^{-1}. Kelly et al.[22] used the relative rate technique to determine $k(Cl+CF_3CH_2CH_2OH)$ relative to $k(Cl+HC(O)OC_2H_5)$ and report $k_{11} = (2.24 \pm 0.04) \times 10^{-11}$ cm^3 $molecule^{-1}$ s^{-1}. As discussed in section 3.1, errors in the reference rate constant are a likely explanation of the overestimation of k_{11} by Kelly et al.[22]

3.4. Relative Rate Study of the Reaction of OH Radicals with $CF_3CH_2CH_2OH$. The kinetics of reaction 12 were measured relative to reactions 9 and 10.

$$OH + CF_3CH_2CH_2OH \rightarrow products \tag{12}$$

The bottom panel in Figure 2 shows the loss of $CF_3CH_2CH_2OH$ versus the loss of the reference compounds following

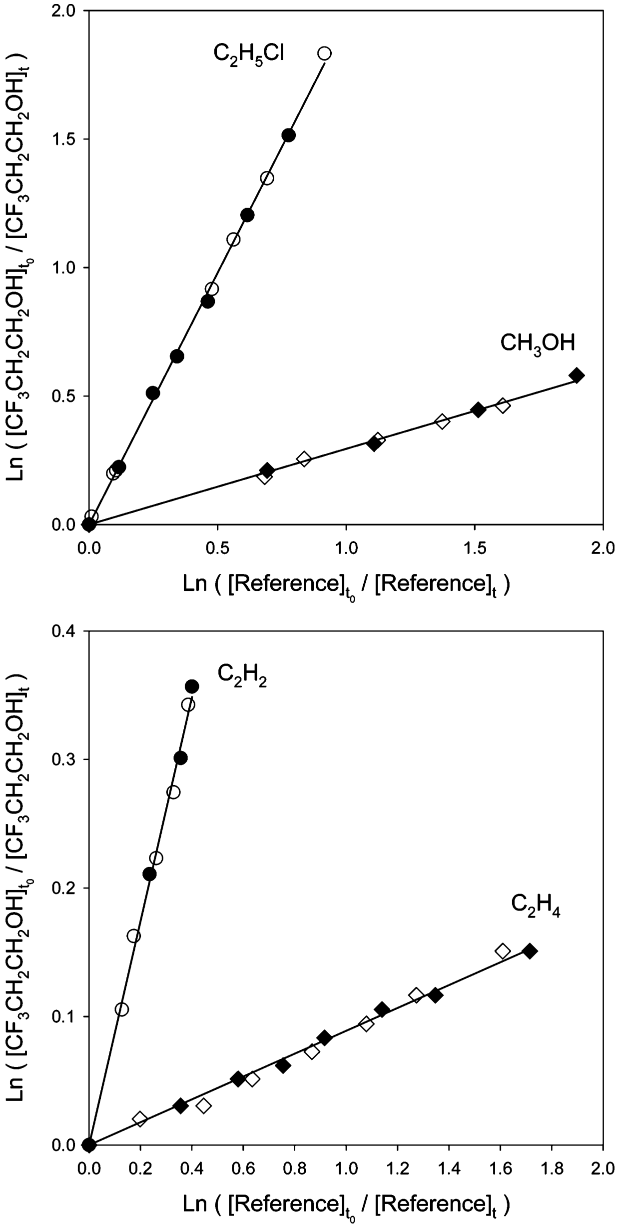

Figure 2. Top panel: loss of $CF_3CH_2CH_2OH$ versus C_2H_5Cl (circles) and CH_3OH (diamonds) following UV irradiation of $CF_3CH_2CH_2OH$/reference/Cl_2 mixtures in 700 Torr of N_2. Bottom panel: loss of $CF_3CH_2CH_2OH$ versus C_2H_2 (circles) and C_2H_4 (diamonds) following UV irradiation of $CF_3CH_2CH_2OH$/reference/CH_3ONO mixtures in 700 Torr of air.

the UV irradiation of $CF_3CH_2CH_2OH$/reference/CH_3ONO mixtures in 700 Torr of air diluent. The lines through the data in Figure 2 are linear least-squares fits to the combined data sets that give $k_{12}/k_9 = 0.87 \pm 0.09$ and $k_{12}/k_{10} = 0.089 \pm 0.010$. Using $k_9 = 7.8 \times 10^{-13}$ [28] and $k_{10} = 7.9 \times 10^{-12}$,[28] we derive $k_{12} = (6.79 \pm 0.70) \times 10^{-13}$ and $(7.03 \pm 0.79) \times 10^{-13}$ cm^3 $molecule^{-1}$ s^{-1}. Results obtained using the two different reference compounds were, within the experimental uncertainties, indistinguishable. We cite a final value for k_{12} that is the average of the two determinations together with error limits that encompass the extremes of the individual determinations, $k_{12} = (6.91 \pm 0.91) \times 10^{-13}$ cm^3 $molecule^{-1}$ s^{-1}. Le Bras et al.[14] used relative rate techniques to determine $k_{12} = (1.06 \pm 0.10) \times 10^{-12}$ cm^3 $molecule^{-1}$ s^{-1}. Kelly et al.[22] used LP-LIF techniques to determine $k_{12} = (8.9 \pm 0.3) \times 10^{-13}$ and relative rate techniques to determine $k_{12} = (1.08 \pm 0.05) \times 10^{-12}$ cm^3 $molecule^{-1}$ s^{-1}. At the present time we are unable to explain the 15−30% difference between k_{12} values measured in the present work and those reported by Le Bras et al.[14] and Kelly et al.[22]

3.5. Determination of the Gas-Phase Dimerization Constant for $CF_3CH_2C(O)OH$. Trifluoropropionic acid, $CF_3CH_2C(O)OH$, is a possible product in the Cl initiated oxidation of $CF_3CH_2C(O)H$, and a calibrated reference spectrum was required for analysis. Carboxylic acids form cyclic dimers[30−32] and the generation of a calibrated reference spectrum required knowledge of the dimerization constant. The observed pressure of $CF_3CH_2C(O)OH$ vapor is expressed as

$$P_{obs} = P_M + P_D = P_M + K_d {P_M}^2 \tag{II}$$

where P_M is the pressure of the monomer, P_D is the pressure of the dimer, and K_d is the dimerization constant. If dimerization occurs in the calibrated volume and the dimer dissociates upon expansion into the chamber, the acid concentration in the chamber will be higher than calculated assuming only the monomer in the calibrated volume. To correct for dimer formation in the calibrated volume, the dimerization constant was determined for trifluoropropionic acid. The procedure used is discussed elsewhere.[32] The dimerization constant for $CF_3CH_2C(O)OH$ was determined to be $K_d = 3.4 \pm 0.3$ $Torr^{-1}$. Crawford et al.[30] measured the dimerization constant of $CH_3C(O)OH$ and report a value of 2.5 ± 0.3 $Torr^{-1}$. LeCrane et al.[33] report the dimerization constant of $CH_3CH_2C(O)OH$ to be 2.9 ± 0.3 $Torr^{-1}$. The extent of dimerization of $CF_3CH_2C(O)OH$ is similar to that in the nonsubstituted acids, presumably reflecting the modest effect of the CF_3 group on electron density distribution in the C(O)OH group.

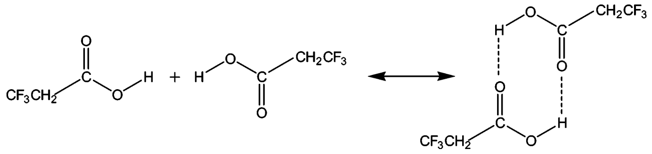

3.6. Products of the Cl Atom Initiated Oxidation of $CF_3CH_2C(O)H$ in 700 Torr of Air. The Cl atom initiated oxidation of $CF_3CH_2C(O)H$ was investigated by irradiating mixtures containing 15−22 mTorr of $CF_3CH_2C(O)H$ and 100 mTorr of Cl_2 in 700 Torr of air diluent. Figure 3 shows spectra acquired before (A) and after (B) a 15 s irradiation of 22.2 mTorr of $CF_3CH_2C(O)H$ and 100 mTorr of Cl_2 in 700 Torr of air. Consumption of $CF_3CH_2C(O)H$ was 18% during irradiation. Panel C shows the IR features of the product spectrum obtained by subtracting $CF_3CH_2C(O)H$ features from panel B. Comparison with the reference spectrum in panel D shows that $CF_3C(O)H$ is an important product. Panel E shows the result of subtracting $CF_3C(O)H$ features from panel C. Comparison of (E) with the reference spectrum in panel F shows that $CF_3CH_2C(O)OH$ is a product. Finally, panel G is the result of stripping $CF_3CH_2C(O)OH$ features from panel E. The residual shown in panel G is due to one, or more, unidentified products. The IR features of this(ese) product(s) scale linearly in all experiments, and its profile follows the pattern expected from a primary product. During this experiment, O_3 was observed as a product at 1043 cm^{-1}. In experiments with a high consumption of $CF_3CH_2C(O)H$, IR features due to CF_3OH, CF_3COOH, $CF_3O_3CF_3$, and COF_2 were also observed.

The observation of $CF_3C(O)H$ and $CF_3CH_2C(O)OH$ as primary products of the Cl initiated oxidation of $CF_3CH_2C(O)H$ is consistent with abstraction of the aldehyde hydrogen

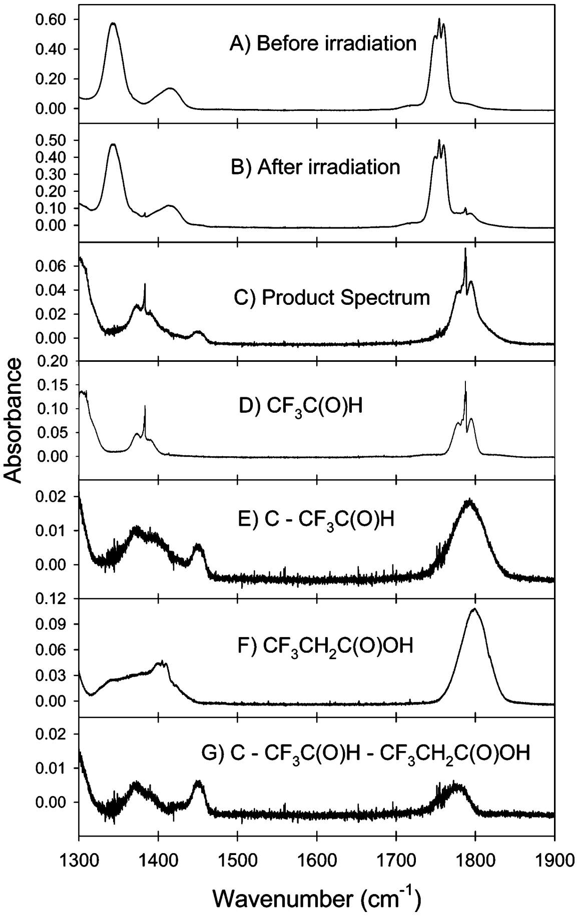

Figure 3. IR spectra obtained before (A) and after (B) a 15 s irradiation of 22.2 mTorr of $CF_3CH_2C(O)H$ and 100 mTorr of Cl_2 in 700 Torr air. (C) shows the IR product spectrum. (E) shows the IR features of the product spectrum after the subtraction of features due to $CF_3C(O)H$. (G) shows the residual IR features of the product spectrum after the subtraction of features due to $CF_3C(O)H$ and $CF_3CH_2C(O)OH$.

followed by reaction with oxygen to form the acyl peroxy radical, $CF_3CH_2C(O)O_2$.

$$CF_3CH_2C(O)H + Cl \rightarrow CF_3CH_2C(O) + HCl \quad (5a)$$

$$CF_3CH_2C(O) + O_2 \rightarrow CF_3CH_2C(O)OO \quad (13)$$

The acyl peroxy radical, $CF_3CH_2C(O)OO$, reacts with other peroxy radicals to form the radical, $CF_3CH_2C(O)O$.

$$CF_3CH_2C(O)OO + RO_2 \rightarrow CF_3CH_2C(O)O + RO + O_2 \quad (14)$$

$CF_3CH_2C(O)O$ eliminates CO_2 to form the alkyl radical, CF_3CH_2, which will add O_2 and react with other peroxy radicals to give the alkoxy radical, CF_3CH_2O.

$$CF_3CH_2C(O)O \rightarrow CF_3CH_2 + CO_2 \quad (15)$$

$$CF_3CH_2 + O_2 \rightarrow CF_3CH_2OO \quad (16)$$

$$CF_3CH_2OO + RO_2 \rightarrow CF_3CH_2O + RO + O_2 \quad (17)$$

Finally, the alkoxy radical, CF_3CH_2O, reacts with oxygen to give the observed product, $CF_3C(O)H$.

$$CF_3CH_2O + O_2 \rightarrow CF_3C(O)H + HO_2 \quad (18)$$

Analogous to studies of fluorinated aldehydes by Sulbaek Andersen et al.,[34,35] the reaction of $CF_3CH_2C(O)O_2$ radicals with HO_2 radicals (formed as a product in reaction 18) is expected to proceed via three channels

$$CF_3CH_2C(O)OO + HO_2 \rightarrow CF_3CH_2C(O)OH + O_3 \quad (19a)$$

$$CF_3CH_2C(O)OO + HO_2 \rightarrow CF_3CH_2C(O)OOH + O_2 \quad (19b)$$

$$CF_3CH_2C(O)OO + HO_2 \rightarrow CF_3CH_2C(O)O + OH + O_2 \quad (19c)$$

The $CF_3CH_2C(O)O$ radical produced in reaction 19c will then react via reaction steps (15)−(18) to form $CF_3C(O)H$.

$CF_3C(O)H$, $CF_3CH_2C(O)OH$, and $CF_3CH_2C(O)OOH$ are formed as primary products following the Cl atom initiated oxidation of $CF_3CH_2C(O)H$ in air. These primary products react with Cl atoms to form secondary products.

$$CF_3C(O)H + Cl \rightarrow \text{products} \quad (20)$$

$$CF_3CH_2C(O)OH + Cl \rightarrow \text{products} \quad (21)$$

$$CF_3CH_2C(O)OOH + Cl \rightarrow \text{products} \quad (22)$$

The concentration profile of the reactive primary product, $CF_3C(O)H$, can be described by the expression[36]

$$\frac{[CF_3C(O)H]}{[CF_3CH_2C(O)H]_0} = \frac{\alpha(1-x)\{(1-x)^{(k_{20}/k_5)-1} - 1\}}{\{1-(k_{20}/k_5)\}} \quad (III)$$

where $x = 1 - ([CF_3CH_2C(O)H]/[CF_3CH_2C(O)H]_0)$ is the fractional consumption of $CF_3CH_2C(O)H$, and α is the yield of $CF_3C(O)H$ from reaction of Cl atoms with $CF_3CH_2C(O)H$ in the presence of oxygen. Similarly, the concentration profile of the reactive primary product, $CF_3CH_2C(O)OH$, can be described by the expression

$$\frac{[CF_3CH_2C(O)OH]}{[CF_3CH_2C(O)H]_0} = \frac{\beta(1-x)\{(1-x)^{(k_{21}/k_5)-1} - 1\}}{\{1-(k_{21}/k_5)\}} \quad (IV)$$

where β is the yield of $CF_3CH_2C(O)OH$ from reaction of Cl atoms with $CF_3CH_2C(O)H$ in the presence of oxygen.

Figure 4 shows a plot of [primary products]/$[CF_3CH_2C(O)H]_0$ versus $\Delta[CF_3CH_2C(O)H]/[CF_3CH_2C(O)H]_0$ for three experiments in which $CF_3CH_2C(O)H/Cl_2$ mixtures in 700 Torr of air diluent were subjected to successive irradiations. The formation of products and the loss of $CF_3CH_2C(O)H$ have been normalized to the initial $CF_3CH_2C(O)H$ concentration. A fit of eq III to the $CF_3C(O)H$ data gives $\alpha = 0.76 \pm 0.05$ and $k_{20}/k_5 = 0.17 \pm 0.03$. A fit of eq IV to the $CF_3CH_2C(O)OH$ data gives $\beta = 0.14 \pm 0.01$ and $k_{21}/k_5 = 0.033 \pm 0.016$. Also shown in Figure 4 is the unknown product whose IR spectral features are shown in Figure 3G.

Although we cannot positively identify the unknown shown in Figure 3G, there are four pieces of information that lead us to believe that the unknown is the peracid, $CF_3CH_2C(O)OOH$. First, the IR features scale linearly in all experiments (suggesting they are associated with one compound). Second, the formation of IR features follows the pattern expected from a primary product. Third, the IR features have frequencies consistent with those expected from $CF_3CH_2C(O)OOH$. Figure 5 shows a comparison of the IR spectrum of the unknown (5A) with $CH_3CH_2C(O)OOH$ (5B) and $CF_3C(O)OOH$ (5C) at 1300−1900 cm^{-1}. The spectra have similar features at ~1450 cm^{-1} (OH bend) and ~1790 cm^{-1} (carbonyl stretch). The IR spectrum of

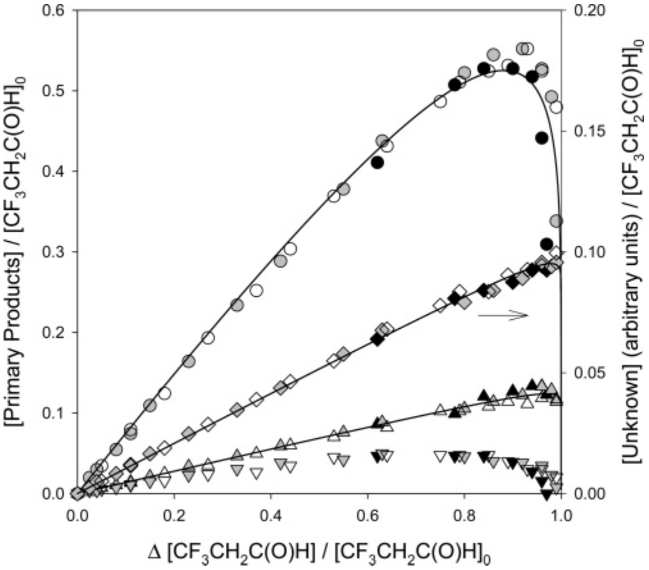

Figure 4. Formation of primary products versus loss of $CF_3CH_2C(O)H$, normalized for the initial aldehyde concentration, for three experiments in which $CF_3CH_2C(O)H/Cl_2$ mixtures were irradiated in 700 Torr of air. The primary products are $CF_3C(O)H$ (circles), $CF_3CH_2C(O)OH$ (triangles up), ozone (triangles down) and an unknown (diamonds).

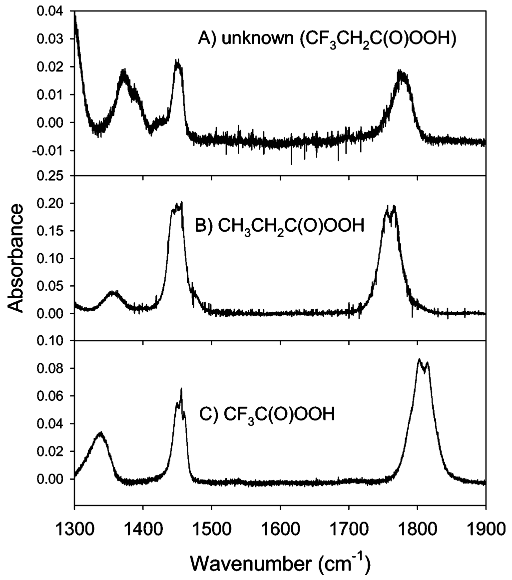

Figure 5. IR spectrum of the unknown (A), $CH_3CH_2C(O)OOH$ (B), and $CF_3C(O)OOH$ (C).

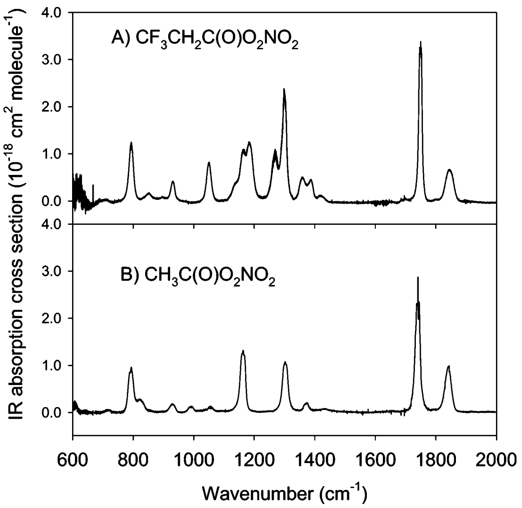

Figure 6. IR spectra of $CF_3CH_2C(O)O_2NO_2$ (A) and $CH_3C(O)O_2NO_2$ (B).

the unknown is consistent with its assignment as the peracid, $CF_3CH_2C(O)OOH$. Fourth, given the observation of $CF_3CH_2C(O)OH$ and O_3 as products of reaction 19a, it would be expected, by analogy to the oxidation mechanism of fluorinated aldehydes,[34,35] that the peracid will also be formed in the system. In the absence of a calibrated reference spectrum, it is not possible to quantify the peracid yield at the present time; however, because the yield of $CF_3C(O)H$ is 0.76 and the yield of $CF_3CH_2C(O)OH$ is 0.14, carbon balance requires that the yield of $CF_3CH_2C(O)OOH$ is ≤ 0.10. The peracid yields given in Figure 4 are in arbitrary units. Kelly et al.[22] carried out experiments to determine the products formed from the OH and Cl initiated oxidation of $CF_3CH_2C(O)H$. The major product observed was $CF_3C(O)H$, formed with a yield close to unity. Kelly et al.[22] found no evidence for the formation of either $CF_3CH_2C(O)OH$ or $CF_3CH_2C(O)OOH$. Comparing Figure 3E and 3G in the present work with Figures 5 and 6 from Kelly et al.[22] indicates that the noise on the IR spectra was substantially (approximately an order of magnitude) lower in the present work. This factor, together with the lower spectral resolution (1.0 compared to 0.25 cm^{-1}) and the use of $ClC(O)C(O)Cl$ as a Cl atom source, which leads to CCl_2O formation and obscures the carbonyl stretching region, may explain why Kelly et al.[22] did not observe $CF_3CH_2C(O)OH$ or $CF_3CH_2C(O)OOH$ in their study.

3.7. Infrared Spectrum of $CF_3CH_2C(O)O_2NO_2$. The IR spectrum of $CF_3CH_2C(O)O_2NO_2$ was recorded by irradiating a mixture of 15.3 mTorr of $CF_3CH_2C(O)H$, 101 mTorr of Cl_2 and 10.9 mTorr of NO_2 in 700 Torr of air. The reaction of Cl atoms with $CF_3CH_2C(O)H$ in the presence of O_2 leads to the formation of trifluoropropionyl peroxy radicals. By analogy to the behavior of other acyl peroxy radicals, it is expected that trifluoropropionyl peroxy radicals will react rapidly with NO_2 to give peroxy trifluoropropionyl nitrate, $CF_3CH_2C(O)O_2NO_2$.

$$CF_3CH_2C(O)H + Cl \rightarrow CF_3CH_2C(O) + HCl \quad (5a)$$

$$CF_3CH_2C(O) + O_2 \rightarrow CF_3CH_2C(O)OO \quad (23)$$

$$CF_3CH_2C(O)OO + NO_2 \leftrightarrow CF_3CH_2C(O)O_2NO_2 \quad (24)$$

Acyl peroxy nitrates are thermally unstable and decompose to re-form acyl peroxy radicals and NO_2. In the presence of excess NO_2 thermal decomposition of $CF_3CH_2C(O)O_2NO_2$ is masked by its re-formation via reaction 25. Following UV irradiation of $CF_3CH_2C(O)H/Cl_2/NO_2$/air mixtures, a product was observed with IR features at 794, 931, 1050, 1175, 1267, 1300, 1359, 1387, 1750, and 1845 cm^{-1} whose spectrum is shown in Figure 6A. The features shown in Figure 6A increased linearly with loss of $CF_3CH_2C(O)H$. The product features at 794, 1300, 1750, and 1845 cm^{-1} are characteristic of the NO scissors, NO_2 symmetric stretch, NO_2 asymmetric stretch, and CO stretching modes in acyl peroxy nitrates and we ascribe the spectrum in Figure 6A to $CF_3CH_2C(O)O_2NO_2$. For comparison, the spectrum of $CH_3C(O)O_2NO_2$ is shown in Figure 6B.

The addition of NO to mixtures containing $CF_3CH_2C(O)O_2NO_2$ results in a slow decay of the peroxy nitrate due to a competition between the following reactions:

$$CF_3CH_2C(O)OO + NO_2 \leftrightarrow CF_3CH_2C(O)O_2NO_2 \quad (24)$$

$$CF_3CH_2C(O)OO + NO \rightarrow CF_3CH_2C(O)O + NO_2 \quad (25)$$

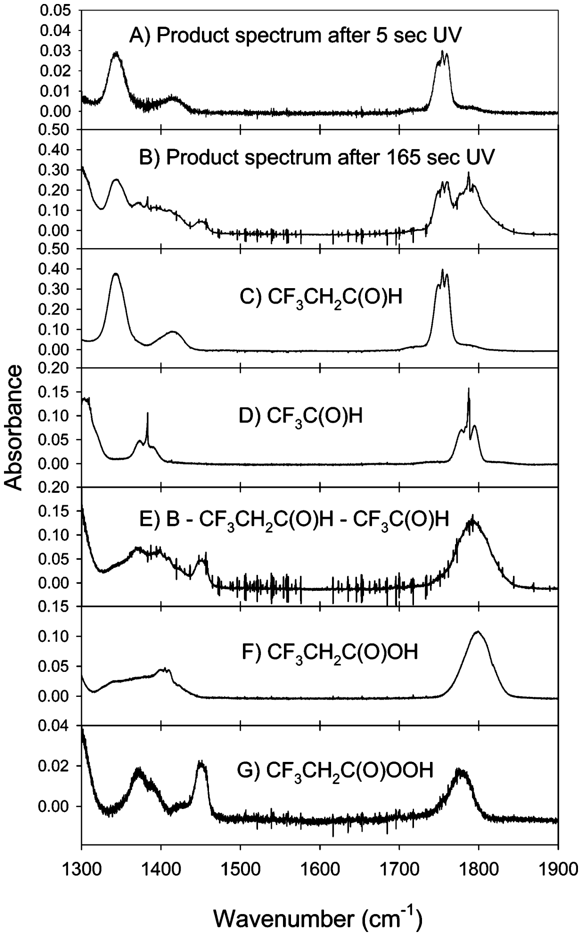

Figure 7. Product IR spectra obtained after 5 s (A) and after 165 s (B) irradiation of 29.8 mTorr of $CF_3CH_2CH_2OH$ and 100 mTorr of Cl_2 in 700 Torr air. (E) shows the product IR spectrum (B) after removal of IR features due to $CF_3CH_2C(O)H$ and $CF_3C(O)H$.

followed by decomposition of $CF_3CH_2C(O)O$

$$CF_3CH_2C(O)O \rightarrow CF_3CH_2 + CO_2 \tag{15}$$

Calibration of $CF_3CH_2C(O)O_2NO_2$ was achieved by equating the loss of the peroxy nitrate to the formation of CO_2 observed in such experiments. The integrated band strength (1700−1777 cm^{-1}) of the NO_2 asymmetric stretching feature in $CF_3CH_2C(O)O_2NO_2$ determined herein is 5.16×10^{-17}, which is indistinguishable from that of $(5.14 \pm 0.10) \times 10^{-17}$ cm^2 molecule^{-1} cm^{-1} for the corresponding feature in $CH_3C(O)O_2NO_2$.[37] The integrated band strengths of the corresponding feature in $CF_3(CF)_nC(O)O_2NO_2$ have been determined to be $(5.15 \pm 1.03) \times 10^{-17}$, $(5.25 \pm 1.04) \times 10^{-17}$, $(5.56 \pm 1.11) \times 10^{-17}$, and $(5.53 \pm 1.11) \times 10^{-17}$ cm^2 molecule^{-1} cm^{-1} for $n = 0-3$, respectively.[38,39] The intensity of the NO_2 asymmetric stretch at 1700−1780 cm^{-1} in $RC(O)O_2NO_2$ molecules appears to be insensitive to the nature of the R group.

3.8. Product Study of the Cl + $CF_3CH_2CH_2OH$ Reaction in 700 Torr of Air. The Cl atom initiated oxidation of $CF_3CH_2CH_2OH$ was investigated by irradiating mixtures containing 15−30 mTorr of $CF_3CH_2CH_2OH$ and 100 mTorr of Cl_2 in 700 Torr of air diluent. Figure 7 shows product spectra acquired after a 5 s irradiation (A) and after a 165 s irradiation (B) of 29.8 mTorr $CF_3CH_2CH_2OH$ and 100 mTorr Cl_2 in 700 Torr of air. Panels C, D, F, and G show reference spectra for $CF_3CH_2C(O)H$, $CF_3C(O)H$, $CF_3CH_2C(O)OH$, and $CF_3CH_2C(O)OOH$, respectively. Consumption of $CF_3CH_2CH_2OH$ was 4% during the 4 s irradiation and 78% during the 165 s irradiation. Comparison of the spectrum in (A) with the reference spectrum in (C) indicates that $CF_3CH_2C(O)H$ is the major primary product. After subtraction of features attributable to $CF_3CH_2C(O)H$ from panel (A), there were no residual features that could be attributed to carbon containing products. In all experiments employing low $CF_3CH_2CH_2OH$ consumptions (<10%), $CF_3CH_2C(O)H$ was the only observed product. We conclude that $CF_3CH_2C(O)H$ is the sole primary oxidation product of $CF_3CH_2CH_2OH$.

This conclusion is consistent with recent work by Hurley et al.[40] in which the chlorine initiated oxidation of $CF_3(CF_2)_nCH_2OH$ ($n = 0-3$) was shown to give one primary product: $CF_3(CF_2)_nC(O)H$ ($n = 0-3$). Hurley et al.[18] have also shown that $CF_3(CF_2)_3CH_2C(O)H$ is the sole primary product of the Cl initiated oxidation of the fluorotelomer alcohol, $CF_3(CF_2)_3CH_2CH_2OH$. The reaction of Cl atoms with fluorinated alcohols is believed to proceed predominantly (>90%) via attack at the CH_2 group α to the alcohol functionality to give an α-hydroxyalkyl radical.[10] The selectivity of the Cl atom attack arises from a combination of the deactivating effect of fluorine substituents and the activating effect of the alcohol substituent on the CH_2 groups in the molecule.[40] The atmospheric fate of α-hydroxyalkyl radicals is believed to be reaction with O_2 to give the corresponding aldehydes. The initial steps in the chlorine initiated oxidation of $CF_3CH_2CH_2OH$ are then

$$CF_3CH_2CH_2OH + Cl \rightarrow CF_3CH_2CHOH + HCl \tag{11a}$$

$$CF_3CH_2CHOH + O_2 \rightarrow CF_3CH_2C(O)H + HO_2 \tag{26}$$

$$CF_3CH_2C(O)H + Cl \rightarrow \text{products} \tag{5}$$

The concentration profile of the reactive primary product, $CF_3CH_2C(O)H$, can be described[36] by the expression

$$\frac{[CF_3CH_2C(O)H]}{[CF_3CH_2CH_2C(O)H]_0} = \frac{\gamma(1-x)\{(1-x)^{(k_5/k_{11})-1} - 1\}}{\{1 - (k_5/k_{11})\}} \tag{V}$$

where $x = 1 - ([CF_3CH_2CH_2OH]/[CF_3CH_2CH_2OH]_0)$ is the fractional consumption of $CF_3CH_2CH_2OH$ and γ is the yield of $CF_3CH_2C(O)H$ from reaction of Cl atoms with $CF_3CH_2CH_2OH$ in the presence of oxygen. Figure 8 shows a plot of $[CF_3CH_2C(O)H]/[CF_3CH_2CH_2OH]_0$ versus $\Delta[CF_3CH_2CH_2OH]/[CF_3CH_2CH_2OH]_0$ for four experiments in which mixtures of $CF_3CH_2C(O)H$ and chlorine in 700 Torr of air diluent received successive UV irradiations. Product formation and $CF_3CH_2CH_2OH$ loss have been normalized to the initial $CF_3CH_2CH_2OH$ concentration. A fit of eq V to the combined $CF_3CH_2C(O)H$ data gives $\gamma = 1.06 \pm 0.06$ and $k_5/k_{11} = 1.33 \pm 0.12$. Using the rate constants derived from the relative rate measurements in this work, the rate constant ratio is $k_5/k_{11} = (1.81 \pm 0.27)$ x $10^{-11}/(1.59 \pm 0.19) \times 10^{-11} = 1.14 \pm 0.22$. The rate constant ratio derived from the fit to eq V is in agreement with that derived from the individual rate constant measurements, providing confidence in the present methodology.

Comparison of Figure 7B with the reference spectrum of $CF_3C(O)H$ in Figure 7D shows the formation of $CF_3C(O)H$ as a secondary oxidation product in this system. Figure 7E shows the result of subtracting $CF_3CH_2C(O)H$ and $CF_3C(O)H$ features from Figure 7B. Comparison of Figure 7E with reference spectra of $CF_3CH_2C(O)OH$ (7F) and $CF_3CH_2C(O)OOH$ (7G) shows those compounds to be present also. The observation of $CF_3C(O)H$, $CF_3CH_2C(O)OH$ and $CF_3CH_2C(O)OOH$ as second-

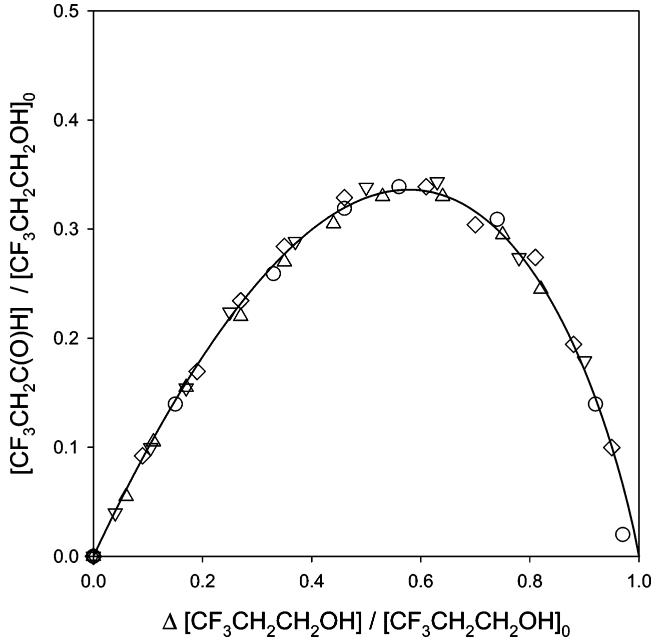

Figure 8. Formation of the primary product $CF_3CH_2C(O)H$ versus loss of $CF_3CH_2CH_2OH$, normalized for the initial alcohol concentration, for four experiments in which $CF_3CH_2CH_2OH/Cl_2$ mixtures were irradiated in 700 Torr of air.

ary oxidation products from the chlorine initiated oxidation of $CF_3CH_2CH_2OH$ is expected considering that $CF_3CH_2C(O)H$ is the sole primary product formed and $CF_3C(O)H$, $CF_3CH_2C(O)OH$ and $CF_3CH_2C(O)OOH$ are observed primary products from the chlorine initiated oxidation of $CF_3CH_2C(O)H$ (see section 3.6). We expect that the observed secondary products will increase linearly with $CF_3CH_2C(O)H$ consumption. Because $CF_3CH_2C(O)H$ is formed in 100% yield from the oxidation of $CF_3CH_2CH_2OH$, $CF_3CH_2C(O)H$ consumption can be equated to the difference between the loss of the parent alcohol and the observed concentration of $CF_3CH_2C(O)H$.

$$\Delta[CF_3CH_2C(O)H] = \Delta[CF_3CH_2CH_2OH] - [CF_3CH_2C(O)H] \quad (VI)$$

Figure 9 shows a plot of the formation of $CF_3C(O)H$, $CF_3CH_2C(O)OH$, and $CF_3CH_2C(O)OOH$ versus the loss of $CF_3CH_2C(O)H$ calculated from eq VI. Product formation and $CF_3CH_2C(O)H$ loss have been normalized to the initial $CF_3CH_2CH_2OH$ concentration. The initial slope of the product profiles in Figure 9 provides information concerning the product yield from the oxidation of $CF_3CH_2C(O)H$. The curvature of the profiles is influenced by the reactivity of the products toward Cl atoms. The lines through the product data in Figure 9 are second-order polynomial least-squares fits to the data. The initial yield of $CF_3C(O)H$ is 0.54 ± 0.03, and the initial yield of $CF_3CH_2C(O)OH$ is 0.30 ± 0.02. In the absence of a calibrated reference spectrum of $CF_3CH_2C(O)OOH$, it is not possible to quantify the peracid yield; however, carbon balance requires its yield to be ≤ 0.16.

The results described above are consistent with those from our recent study of the Cl initiated oxidation of the fluorotelomer alcohol $CF_3(CF_2)_3CH_2CH_2OH$ in the absence of NO_X. We observed $CF_3(CF_2)_3CH_2C(O)H$ as the sole primary product and $CF_3(CF_2)_3C(O)H$, $CF_3(CF_2)_3CH_2C(O)OH$, and $CF_3(CF_2)_3CH_2C(O)OOH$ as secondary products in the oxidation of $CF_3(CF_2)_3CH_2CH_2OH$ in the absence of NO_X.[18]

Kelly et al.[22] studied the products of the OH radical and Cl atom initiated oxidation of $CF_3CH_2CH_2OH$ in indoor and outdoor chambers in the absence of NO_X. Kelly et al.[22] report $CF_3CH_2C(O)H$ as the sole primary product. In the absence of NO_X the major degradation product of $CF_3CH_2C(O)H$ is $CF_3C(O)H$ and the combined yield of the two aldehydes formed from $CF_3CH_2CH_2OH$ was close to unity. They found no evidence for the formation of $CF_3CH_2C(O)OH$ or $CF_3CH_2C(O)OOH$ in the IR product spectra. A possible explanation for why Kelly et al.[22] did not observe $CF_3CH_2C(O)OH$ or $CF_3CH_2C(O)OOH$ is discussed at the end of section 3.6.

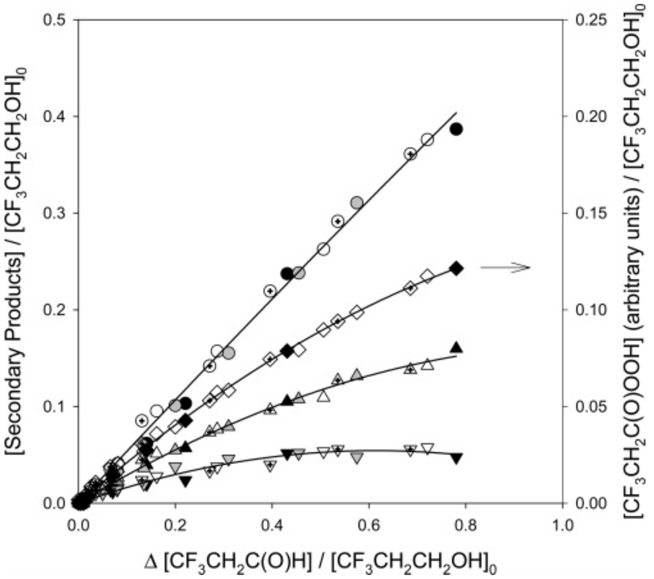

Figure 9. Formation of secondary products versus the loss of $CF_3CH_2C(O)H$, normalized for the initial alcohol concentration, for four experiments in which $CF_3CH_2CH_2OH/Cl_2$ mixtures were irradiated in 700 Torr of air. The secondary products are $CF_3C(O)H$ (circles), $CF_3CH_2C(O)OH$ (triangles up), ozone (triangles down), and $CF_3CH_2C(O)OOH$ (diamonds).

3.9. Product Study of the Cl + $CF_3CH_2CH_2OH$ Reaction in the Presence of NO_X. The mechanism of Cl atom initiated oxidation of $CF_3CH_2CH_2OH$ in the presence of NO_X was investigated by irradiating a mixture of 15 mTorr of $CF_3CH_2CH_2OH$, 91.8 mTorr of NO, and 98.5 mTorr of Cl_2 in 700 Torr of air diluent. Figure 10 shows a plot of the observed formation of $CF_3CH_2C(O)H$, HC(O)OH and $CF_3C(O)H$ versus loss of $CF_3CH_2CH_2OH$ for successive UV irradiations. As seen from Figure 10, the concentration of HC(O)OH increased linearly with $CF_3CH_2CH_2OH$ loss, whereas the concentration of $CF_3C(O)H$ starts at a very low level and curves upward with $CF_3CH_2CH_2OH$ loss. Such behavior indicates that HC(O)OH is a primary product and that $CF_3C(O)H$ is both a primary and a secondary product in the system. As with the experiments in the absence of NO_X, the concentration of $CF_3CH_2C(O)H$ increases for small consumptions of $CF_3CH_2CH_2OH$ and then decreases at larger consumptions. This behavior suggests that $CF_3CH_2C(O)H$ is a primary product in the Cl atom initiated oxidation of $CF_3CH_2CH_2OH$ but is lost via secondary reaction with Cl atoms at higher conversions of $CF_3CH_2CH_2OH$. In experiments conducted in the absence of NO_X, there was one primary product, $CF_3CH_2C(O)H$, in a yield that was indistinguishable from 100%. In the presence of NO_X, $CF_3CH_2C(O)H$ is the major, but not the sole, primary product. Formation of HC(O)OH as a primary product in the presence of NO_X is significant given the absence of this species as either a primary or secondary product in experiments conducted in the absence of NO_X. It is clear that the presence of NO_X has a substantial impact on the first step of the oxidation mechanism of $CF_3CH_2CH_2OH$.

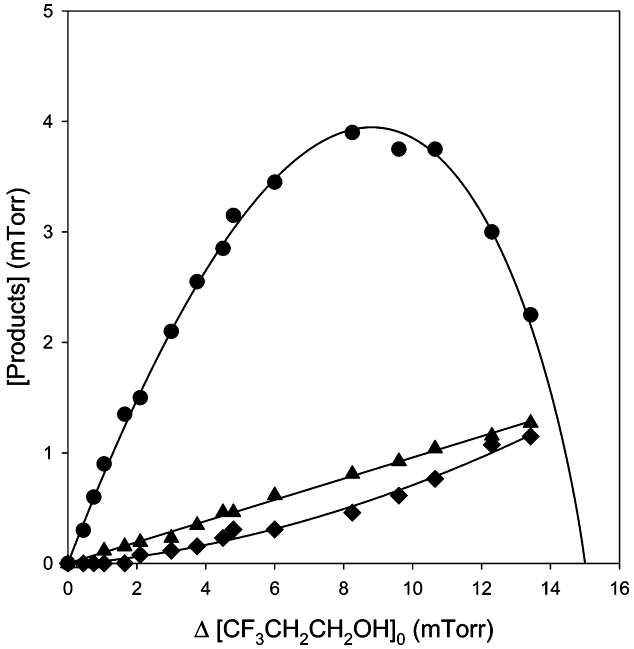

Figure 10. Primary product formation versus $CF_3CH_2CH_2OH$ loss for successive irradiations of a mixture of 15 mTorr of $CF_3CH_2CH_2OH$, 91.8 mTorr of NO and 98.5 mTorr of Cl_2 in 700 Torr air. The primary products are $CF_3CH_2C(O)H$ (circles), HC(O)OH (triangles), and $CF_3C(O)H$, (diamonds).

Sulbaek Andersen et al.[41] have reported the results of a study of the Cl initiated oxidation of the 4:2 fluorotelomer alcohol, $CF_3(CF_2)_3CH_2CH_2OH$, in the presence of NO_X. In the presence of NO_X, $CF_3(CF_2)_3CH_2C(O)H$, HC(O)OH, and $CF_3(CF_2)_3C(O)H$ were formed as primary products in yields of 44%, 52%, and 21%, respectively. In contrast, in the absence of NO_X the Cl initiated oxidation of $CF_3(CF_2)_3CH_2CH_2OH$ gave a sole primary product, $CF_3(CF_2)_3CH_2C(O)H$.[18] These results were used to construct a mechanism in which Cl atoms react with $CF_3(CF_2)_3CH_2CH_2OH$ to give $CF_3(CF_2)_3CH_2CHOH$ radicals that then add O_2 to give chemically activated α-hydroxy peroxy radicals designated as $[CF_3(CF_2)_3CH_2CHOH(OO)]^*$. Approximately 50% of the $[CF_3(CF_2)_3CH_2CHOH(OO)]^*$ radicals decompose "promptly" (on a time scale less than the collisional time scale of approximately 10^{-10} s) to give HO_2 radicals and $CF_3(CF_2)_3CH_2C(O)H$. The remaining $[CF_3(CF_2)_3CH_2CHOH(OO)]^*$ radicals undergo collisional deactivation to give thermalized peroxy radicals, $CF_3(CF_2)_3CH_2CHOH(OO)$. Decomposition to HO_2 and $CF_3(CF_2)_3CH_2C(O)H$ is the dominant atmospheric fate of the thermalized α-hydroxy peroxy radicals. In the presence of excess NO, the thermalized peroxy radicals react to give $CF_3(CF_2)_3CH_2CHOH(O)$ radicals that then decompose to give HC(O)OH and the alkyl radical $CF_3(CF_2)_3CH_2$. Secondary products included $CF_3(CF_2)_3CH_2C(O)O_2NO_2$, $CF_3(CF_2)_3C(O)O_2NO_2$, and COF_2. In contrast to experiments conducted in the absence of NO_X, there was no evidence (<2% yield) for the formation of the perfluorinated acid $CF_3(CF_2)_3C(O)OH$.

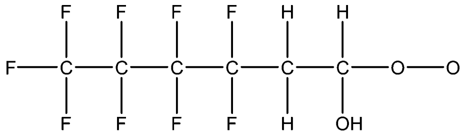

$$F{-}CF_2{-}CF_2{-}CF_2{-}CF_2{-}CH_2{-}CH(OH){-}O{-}O$$

It seems reasonable to assume that a similar mechanism explains the formation of HC(O)OH and $CF_3C(O)H$ as primary products in the chlorine initiated oxidation of $CF_3CH_2CH_2OH$ in the presence of NO_X. CF_3CH_2CHOH radicals react with O_2 to give chemically excited peroxy radicals

$$CF_3CH_2CH_2OH + Cl \rightarrow CF_3CH_2CHOH + HCl \quad (11a)$$

$$CF_3CH_2CHOH + O_2 \rightarrow [CF_3CH_2CHOH(OO)]^* \quad (27)$$

There are two possible fates of $[CF_3CH_2CHOH(OO)]^*$: (i) "prompt" decomposition to give HO_2 radicals and $CF_3CH_2C(O)H$ via reaction 28 and (ii) collisional deactivation to give thermalized $CF_3CH_2CHOH(OO)$ radicals via reaction 29.

$$[CF_3CH_2CHOH(OO)]^* \rightarrow CF_3CH_2C(O)H + HO_2 \quad (28)$$

$$[CF_3CH_2CHOH(OO)]^* + M \rightarrow CF_3CH_2CHOH(OO) + M \quad (29)$$

There are two possible fates of thermalized $CF_3CH_2CHOH(OO)$ radicals. $CF_3CH_2CHOH(OO)$ radicals can decompose via reaction 30 to give HO_2 radicals and $CF_3CH_2C(O)H$, or they can react with NO to form the alkoxy radical, $CF_3CH_2CHOH(O)$, via reaction 31. The alkoxy radical, $CF_3CH_2CHOH(O)$,

$$CF_3CH_2CHOH(OO) \rightarrow CF_3CH_2C(O)H + HO_2 \quad (30)$$

$$CF_3CH_2CHOH(OO) + NO \rightarrow CF_3CH_2CHOH(O) + NO_2 \quad (31)$$

decomposes to give CF_3CH_2 radicals and HC(O)OH.

$$CF_3CH_2CHOH(O) \rightarrow CF_3CH_2 + HC(O)OH \quad (32)$$

The alkyl radical, CF_3CH_2, will react with O_2 and NO to form $CF_3C(O)H$.

$$CF_3CH_2 + O_2 \rightarrow CF_3CH_2OO \quad (33)$$

$$CF_3CH_2OO + NO \rightarrow CF_3CH_2O + NO_2 \quad (34)$$

$$CF_3CH_2O + O_2 \rightarrow CF_3C(O)H + HO_2 \quad (35)$$

The curvature in the product yield plot for $CF_3CH_2C(O)H$ in Figure 10 is attributed to secondary loss of $CF_3CH_2C(O)H$ via reaction with Cl atoms. The concentration profile of the reactive primary product, $CF_3CH_2C(O)H$, can be described[36] by eq V.

A fit of eq V to the $CF_3CH_2C(O)H$ data in Figure 10 gives $\gamma = 0.81 \pm 0.06$ and $k_5/k_{11} = 1.27 \pm 0.12$. The line through the HC(O)OH data in Figure 10 is a linear least-squares fit (forced through zero) giving a molar yield of 9.5 ± 0.3%. The line through the $CF_3C(O)H$ data in Figure 10 is a second-order least-squares fit (forced through zero) giving an initial molar yield of 2 ± 1% $CF_3C(O)H$.

Quoted uncertainties are two standard deviations from the linear regressions together with our estimation of the uncertainties associated with the calibration of our reference spectra. Using the rate constants derived from the relative rate measurements in sections 3.1 and 3.3, the rate constant ratio is $k_5/k_{11} = (1.81 \pm 0.27) \times 10^{-11}/(1.59 \pm 0.20) \times 10^{-11} = 1.14 \pm 0.22$. The value of k_5/k_{11} derived from eq V is consistent with the rate constants measured using the relative rate technique. The presence of NO_X during the Cl initiated oxidation of $CF_3CH_2CH_2OH$ affects the mechanism, diminishing the yield of $CF_3CH_2C(O)H$ by approximately 20%, but does not appear to affect the kinetics of the system.

From the yields of $CF_3CH_2C(O)H$ and HC(O)OH, we conclude that, under ambient conditions, approximately 80% of $[CF_3CH_2CHOH(OO)]^*$ radicals decompose promptly via (28) to give $CF_3CH_2C(O)H$ and that reaction with NO dominates the loss of thermalized $CF_3CH_2CHOH(OO)$ radicals. On the basis of the formation of $CF_3CH_2C(O)H$ and $HC(O)OH$, we can account for (91 ± 3)% of the loss of $CF_3CH_2CH_2OH$ in the initial phase of the degradation.

Given our conclusion that decomposition via reaction 32 is the sole fate of $CF_3CH_2CHOH(O)$ and the expectation that CF_3CH_2 radicals are converted into $CF_3C(O)H$ via reactions 33, 34, and 35, the yields of $HC(O)OH$ and $CF_3C(O)H$ would be expected to be comparable. However, as seen from Figure 10, the initial yield (2%) of $CF_3C(O)H$ is substantially (approximately a factor of 4) lower than that of $HC(O)OH$. It appears that there are other reactions which compete with reaction 35. Under the conditions of this experiment, those reactions include

$$CF_3CH_2O + NO \rightarrow CF_3CH_2ONO \qquad (36)$$

$$CF_3CH_2O + NO_2 \rightarrow CF_3CH_2ONO_2 \qquad (37)$$

The curvature of the $CF_3C(O)H$ profile is consistent with the substantial loss of $CF_3CH_2C(O)H$ via secondary reaction with Cl atoms and the expectation that at least some of this would be converted into $CF_3C(O)H$.

Kelly et al.[22] studied the products arising from the OH radical and Cl atom oxidation of $CF_3CH_2CH_2OH$ conducted in the presence of NO_X. Their results showed that $CF_3CH_2C(O)H$ is the sole primary product and the combined yields of $CF_3CH_2C(O)H$ and $CF_3C(O)H$ were 0.80 ± 0.10. Small unquantified amounts of $CF_3CH_2C(O)O_2NO_2$ were also reported by Kelly et al.[22] These observations are broadly consistent with those of the present work.

3.10. Reaction of O_3 with $CF_3CH_2CH_2OH$. For completeness, an experiment was performed using a mixture of 15 mTorr of $CF_3CH_2CH_2OH$ and 62 mTorr of O_3 in 700 Torr of air diluent at 296 K to check for reaction of O_3 with $CF_3CH_2CH_2OH$. There was no observable (<2%) loss of $CF_3CH_2CH_2OH$ after allowing the mixture to stand in the dark for 90 min, and we derive an upper limit of $k(O_3+CF_3CH_2CH_2OH) < 2 \times 10^{-21}$ cm^3 $molecule^{-1}$ s^{-1}. Assuming this result is representative for fluorotelomer alcohols (FTOHs) and assuming a global background $[O_3] = 40$ ppb, the lifetime of FTOHs with respect to reaction with O_3 will be >5900 days. The lifetime of FTOHs with respect to reaction with OH is approximately 20 days. Reaction with O_3 is not a significant atmospheric fate of FTOHs.

4. Implications for Atmospheric Chemistry

The motivation for the present work was to improve our understanding of the atmospheric chemistry of fluorinated alcohols and assess the likelihood that their atmospheric oxidation contributes to global perfluorocarboxylic acid pollution. The present work provides a detailed description of the kinetics and mechanism of the Cl atom initiated oxidation of $CF_3CH_2CH_2OH$ in the presence and absence of NO_X. Atmospheric oxidation of $CF_3CH_2CH_2OH$ is initiated by reaction with OH radicals. Cl atoms and OH radicals react with $CF_3CH_2CH_2OH$ via the same mechanism (abstraction of a hydrogen atom α to the OH group) and give the same radical products. A study of the Cl atom initiated oxidation of $CF_3CH_2CH_2OH$, therefore, provides information concerning the OH radical initiated atmospheric degradation. Given the structural similarities, the atmospheric oxidation mechanism for $CF_3CH_2CH_2OH$ is likely to be similar to the longer chain, commercially important, fluorotelomer alcohols.

Using results from this and recent work in our laboratories[10,11,18,41] and elsewhere,[14,22] we are able to construct the detailed atmospheric oxidation mechanism for a generic fluorinated alcohol of the structural formula $C_xF_yCH_2CH_2OH$ depicted in Figure 11. Atmospheric oxidation is initiated via reaction with OH radicals. On the basis of the measurement of $k(OH+CF_3CH_2CH_2OH)$ reported here (see section 3.4) and studies of the reactivities of larger members of the series, the atmospheric lifetime of $C_xF_yCH_2CH_2OH$ is estimated to be approximately 10−20 days.[10,14,22] As shown in Figure 11, reaction with OH proceeds via abstraction of the hydrogen α to the −OH group.[10,18,22] The resulting α-hydroxyalkyl radical adds O_2 to give a chemically activated peroxy radical, $[C_xF_yCH_2CHOH(OO)]^*$.[41] These chemically activated peroxy radicals decompose (either promptly or via the intermediacy of the stabilized $C_xF_yCH_2CHOH(OO)$ radical) to give the aldehyde $C_xF_yCH_2C(O)H$.[41]

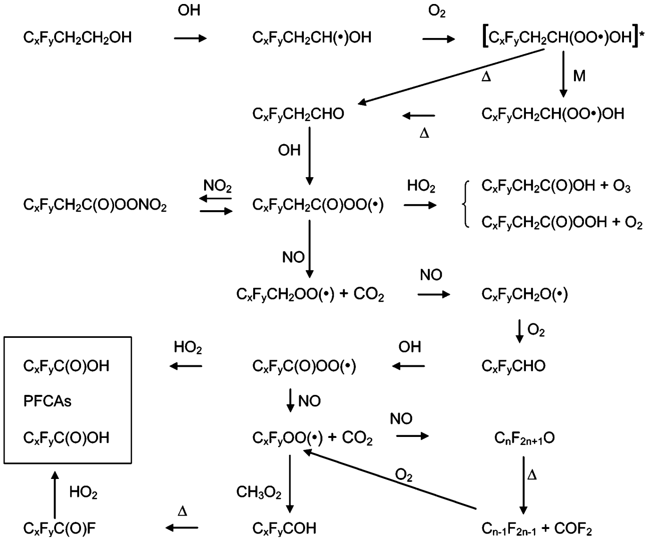

Figure 11. Simplified atmospheric oxidation mechanism for $C_xF_yCH_2CH_2OH$. CH_3O_2 is the most abundant α-hydrogen containing peroxy radical in the atmosphere and was chosen to represent all such peroxy radicals in the reaction leading to C_xF_yOH.

The atmospheric fate of $C_xF_yCH_2C(O)H$ is reaction with OH leading to the formation of $C_xF_yCH_2C(O)O_2$ acyl peroxy radicals. Reaction of $C_xF_yCH_2C(O)O_2$ with NO_2 gives the thermally unstable peroxynitrate $C_xF_yCH_2C(O)O_2NO_2$, which will decompose to regenerate the reactants (see section 3.7). Reaction of $C_xF_yCH_2C(O)O_2$ with HO_2 radicals gives the acid $C_xF_yCH_2C(O)OH$ and peracid $C_xF_yCH_2C(O)OOH$.[42−49] Reaction of $C_xF_yCH_2C(O)O_2$ with NO leads to decarboxylation and the formation of $C_xF_yCH_2O_2$ peroxy radicals. Reaction of $C_xF_yCH_2O_2$ with NO_2 (not shown in Figure 11) gives a very short-lived alkyl peroxy nitrate $C_xF_yCH_2O_2NO_2$ which decomposes rapidly to re-form $C_xF_yCH_2O_2$ and NO_2. Reaction of $C_xF_yCH_2O_2$ with HO_2 (not shown in Figure 11) will give a hydroperoxide $C_xF_yCH_2OOH$. Reaction with OH will return the hydroperoxide to the $C_xF_yCH_2O_2$ radical pool ($C_xF_yCH_2OOH + OH \rightarrow C_xF_yCH_2O_2 + H_2O$). Reaction of $C_xF_yCH_2O_2$ with NO leads to the formation of the perfluoroaldehyde $C_xF_yC(O)H$, as shown in Figure 11.

$C_xF_yC(O)H$ reacts with OH leading to the production of $C_xF_yC(O)O_2$ acyl peroxy radicals. Reaction of $C_xF_yC(O)O_2$ with NO_2 (not shown in Figure 11) gives the thermally unstable peroxynitrate $C_xF_yC(O)O_2NO_2$, which will decompose to regenerate the reactants.[39] Reaction of $C_xF_yC(O)O_2$ with HO_2 radicals gives the acid $C_xF_yC(O)OH$ (see box in Figure 11) and peracid $C_xF_yC(O)OOH$ (not shown in Figure 9).[34,35] Reaction of $C_xF_yC(O)O_2$ with NO leads to decarboxylation and the formation of $C_xF_yO_2$ peroxy radicals, which can react further with NO and initiate a sequence of reactions in which the molecule "unzips" by eliminating COF_2 units indicated by the reactions forming the triangle at the bottom right in Figure 11.[39] $C_xF_yO_2$ radicals can also react with α-hydrogen containing peroxy radicals (CH_3O_2 is by far the most abundant member of this class in the atmosphere and is used for illustration in Figure 11). Reaction of $C_xF_yO_2$ with CH_3O_2 will produce the perfluoro alcohol C_xF_yOH whose sole atmospheric date is elimination of HF giving an acyl fluoride which then hydrolyzes to give a perfluorocarboxylic acid.[11]

The present work confirms that atmospheric oxidation of fluorinated alcohols is a source of perfluorocarboxylic acids in the atmosphere. However, given the competing pathways and complex mechanism illustrated in Figure 11, the magnitude and hence significance of this source is unclear. A modeling study is needed to quantify the contribution of fluorinated alcohol degradation to the environmental perfluorocarboxylic acid burden.

Acknowledgment. We thank Stig Sellevåg (University of Oslo), Claus Nielsen (University of Oslo), and Ole John Nielsen (Copenhagen University) for helpful discussions.

References and Notes

(1) Ellis, D. A.; Moody, C. A.; Mabury, S. A. Trifluoroacetic Acid and Longer Chain Perfluoro Acids, Sources and Analysis. In *Handbook of Environmental Chemistry: Part N, Organofluorines*; Nielson, A.; Ed.; Springer-Verlag: Heidelberg, Germany, 2002; Vol. 3.

(2) Scott, B. F.; Spencer, C.; Moody, C. A.; Mabury, S. A.; MacTavish, D.; Muir, D. C. G. Poster presented at the 13th Annual SETAC Europe Meeting, Hamburg, DE, 2003.

(3) Martin, J. W.; Mabury, S. A.; Solomon, K. R.; Muir, D. C. G. *Environ. Toxicol. Chem.* **2003**, *22*, 196.

(4) Martin, J. W.; Whittle, D. M.; Muir, D. C. G.; Mabury, S. A. *Environ. Sci. Technol*. **2004**, *38*, 5379.

(5) Martin, J. W.; Smithwick, M. M.; Braune, B. M.; Hekstra, P. F.; Muir, D. C. G.; Mabury, S. A. *Environ. Sci. Technol*. **2004**, *38*, 373.

(6) Berthiaume, J.; Wallace, K. B. *Toxicol. Lett*. **2002**, *129*, 23.

(7) Upham, B. L.; Deocampo, N. D.; Wurl, B.; Trosko, J. E. *Int. J. Cancer* **1998**, *78*, 491.

(8) Biegel, L. B.; Hurtt, M. E.; Frame, S. R.; Connor, J. O.; Cook, J. C. *Toxicol. Sci*. **2001**, *60*, 44.

(9) Preliminary risk assessment of the developmental toxicity associated with exposure to perfluorooctanoic acid and its salts; OPPT-2003-0012; US Environmental Protection Agency, Office of Pollution Prevention and Toxics, Risk Assessment Division: Washington, DC, 2003.

(10) Ellis, D. A.; Martin, J. W.; Mabury, S. A.; Hurley, M. D.; Sulbaek Andersen, M. P.; Wallington, T. J. *Environ. Sci. Technol*. **2003**, *37*, 3816.

(11) Ellis, D. A.; Martin, J. W.; De Silva, A. O.; Mabury, S. A.; Hurley, M. D.; Sulbaek Andersen, M. P.; Wallington, T. J. *Environ. Sci. Technol*. **2004**, *38*, 3316.

(12) Martin, J. W.; Muir, D. C. G.; Moody, C. A.; Ellis, D. A.; Kwan, W. C.; Solomon, K. R.; Mabury, S. A. *Anal. Chem*. **2002**, *74*, 584.

(13) Stock, N. L.; Lau, F. K.; Ellis, D. A.; Martin, J. W.; Muir, D. C. G.; Mabury, S. A. *Environ. Sci. Technol*. **2004**, *38*, 991.

(14) Le Bras, G.; Bossoutrot, V.; Magneron, I. Study of the Atmospheric Fate of Fluorinated Alcohols, Final Report to the Fluorotelomer Research Program, July 2003.

(15) Hurley, M. D.; Ball, J. C.; Wallington, T. J.; Sulbaek Andersen, M. P.; Ellis, D. A.; Martin, J. W.; Mabury, S. A. *J. Phys. Chem. A* **2004**, *108*, 5635

(16) Wallington, T. J.; Japar, S. M. J. *Atmos. Chem*. **1989**, *9*, 399.

(17) Atkinson, R. *J. Phys. Chem. Ref. Data* **1989**, Monograph 1.

(18) Hurley, M. D.; Ball, J. C.; Wallington, T. J.; Sulbaek Andersen, M. P.; Ellis, D. A.; Martin, J. W.; Mabury, S. A. *J. Phys. Chem. A* **2004**, *108*, 5635.

(19) Wine, P. H.; Semmes, D. H. *J. Phys. Chem*. **1983**, *87*, 3572.

(20) Bryukov, M. G.; Slagle, I. R.; Knyazev, V. D. *J. Phys. Chem. A* **2003**, *107*, 6565.

(21) Sander, S. P.; Friedl, R. R.; Golden, D. M.; Kurylo, M. J.; Huie, R. E.; Orkin, V. L.; Moortgat, G. K.; Ravishankara, A. R.; Kolb, C. E.; Molina, M. J.; Finlayson-Pitts, B. J. 2003, JPL Publication No. 02-25, NASA Jet Propulsion Laboratory, Pasadena, CA.

(22) Kelly, T.; Bossoutrot, V.; Magneron, I.; Wirtz, K.; Treacy, J.; Mellouki, A.; Sidebottom, H.; Le Bras, G. *J. Phys. Chem. A* **2005**, *109*, 347.

(23) Notario, A.; Le Bras, G.; Mellouki, A. *J. Phys. Chem. A* **1998**, *102*, 3112.

(24) Cavalli, F.; Barnes, I.; Becker, K. H.; Wallington, T. J. *J. Phys. Chem. A* **2000**, *104*, 11310.

(25) Christensen, L. K.; Ball, J. C.; Wallington, T. J. *J. Phys. Chem. A* **2000**, *104*, 345.

(26) Langer, S.; Ljungstrom, E.; Wangberg, I.; Wallington, T. J.; Hurley, M. D.; Nielsen, O. J. *Int. J. Chem. Kinet*. **1996**, *28*, 299.

(27) Wallington, T. J.; Hurley, M. D.; Ball, J. C.; Jenkin, M. E. *Chem. Phys. Lett*. **1993**, *211*, 41.

(28) IUPAC: http://www.iupac-kinetic.ch.cam.ac.uk/.

(29) Sellevåg, S. R.; Kelly, T.; Sidebottom, H.; Nielsen, C. *Phys. Chem. Chem. Phys*. **2004**, *6*, 1243.

(30) Crawford, M. A.; Wallington, T. J.; Szente, J. J.; Maricq, M. M. *J. Phys. Chem. A* **1999**, *103*, 365.

(31) Orlando, J. J.; Tyndall, G. S. *J. Photochem. Photobiol. A: Chem*. **2003**, *157*, 161.

(32) Hurley, M. D.; Sulbaek Andersen, M. P.; Wallington, T. J.; Ellis, D. A.; Martin, J. W.; Mabury, S. A. *J. Phys. Chem. A* **2004**, *108*, 615.

(33) Le Crâne, J. P.; Villenave, E.; Hurley, M. D.; Wallington, T. J.; Ball, J. C. *J. Phys. Chem. A*, submitted.

(34) Sulbaek Andersen, M. P.; Hurley, M. D.; Wallington, T. J.; Ball, J. C.; Martin, J. W.; Ellis, D. A.; Mabury, S. A. *Chem. Phys. Lett*. **2003**, *381*, 14.

(35) Sulbaek Andersen, M. P.; Stenby, C.; Nielsen, O. J.; Hurley, M. D.; Ball, J. C.; Wallington, T. J.; Martin, J. W.; Ellis, D. A.; Mabury, S. A. *J. Phys. Chem. A* **2004**, *108*, 6325.

(36) Meagher, R. J.; McIntosh, M. E.; Hurley, M. D.; Wallington, T. J. *Int. J. Chem. Kinet*. **1997**, *29*, 619.

(37) Tsalkani, N.; Toupance, G.. *Atmos. Environ*. **1989**, *23*, 1849.

(38) Sulbaek Andersen, M. P.; Hurley, M. D.; Wallington, T. J.; Ball, J. C.; Martin, J. W.; Ellis, D. A.; Mabury, S. A.; Nielsen, O. J. *Chem. Phys. Lett*. **2003**, *379*, 28.

(39) Sulbaek Andersen, M. P.; Nielsen, O. J.; Hurley, M. D.; Ball, J. C.; Wallington, T. J.; Stevens, J. E.; Martin, J. W.; Ellis, D. A.; Mabury, S. A. *J. Phys. Chem A* **2004**, *108*, 5189.

(40) Hurley, M. D.; Wallington, T. J.; Sulbaek Andersen, M. P.; Ellis, D. A.; Martin, J. W.; Mabury, S. A. *J. Phys. Chem. A* **2004**, *108*, 1973.

(41) Sulbaek Andersen, M. P.; Nielsen, O. J.; Hurley, M. D.; Ball, J. C.; Wallington, T. J.; Ellis, D. A.; Martin, J. W.; Mabury, S. A. *J. Phys. Chem. A* **2005**, *109*, 1849.

(42) Niki, H.; Maker, P. D.; Savage, C. M.; Breitenbach, L. P. *J. Phys. Chem*. **1985**, *89*, 588.

(43) Moortgat, G. K.; Veyret, B.; Lesclaux, R. *Chem. Phys. Lett.* **1989**, *160*, 443.

(44) Horie, O.; Moortgat, G. K. *J. Chem. Soc., Faraday Trans.* **1992**, *88*, 3305.

(45) Crawford, M. A.; Wallington, T. J.; Szente, J. J.; Maricq, M. M.; Francisco, J. S. *J. Phys. Chem. A* **1999**, *103*, 365.

(46) Atkinson, R.; Baulch, D. L.; Cox, R. A.; Hampson, R. F.; Kerr, J. A.; Rossi, M. J.; Troe, J. *Evaluated kinetic and photochemical data for atmospheric chemistry, Organic species: Supplement VII, Journal of Physical and Chemical Reference Data* **1999**, *28*, 391.

(47) Atkinson, R. *Atmos. Environ.* **2000**, *34*, 2063.

(48) Tomas, A.; Villenave, E.; Lesclaux, R. *J. Phys. Chem. A* **2001**, *105*, 3505.

(49) Hasson, A. S.; Tyndall, G. S.; John J. Orlando, J. J. *J. Phys. Chem. A* **2004**, *108*, 5979.